**Citation: Molecular Therapy–Nucleic Acids (2013) 2, e96;** doi:10.1038/mtna.2013.22

www.nature.com/mtna

# Efficient Biodistribution and Gene Silencing in the Lung epithelium via Intravenous Liposomal Delivery of siRNA

**Jana McCaskill[1], Richa Singhania[1], Melinda Burgess[1], Rachel Allavena[2], Sherry Wu[2], Antje Blumenthal[1,4] and Nigel AJ McMillan[1,5]**

**RNA interference (RNAi) may provide a therapeutic solution to many pulmonary epithelium diseases. However, the main barrier to the clinical use of RNAi remains the lack of efficient delivery vectors. Research has mainly concentrated on the intranasal route of delivery of short interfering RNA (siRNA) effector molecules for the treatment of respiratory diseases. However, this may be complicated in a diseased state due to the increased fluid production and tissue remodeling. Therefore, we investigated our hydration of a freeze-dried matrix (HFDM) formulated liposomes for systemic delivery to the lung epithelium. Here, we show that 45 ± 2% of epithelial murine lung cells receive siRNA delivery upon intravenous (IV) liposomal administration. Furthermore, we demonstrate that liposomal siRNA delivery resulted in targeted gene and protein knockdown throughout the lung, including lung epithelium. Taken together, this is the first description of lung epithelial delivery via cationic liposomes, and provides a proof of concept for the use of IV liposomal RNAi delivery to specifically knockdown targeted genes in the respiratory system. This approach may provide an attractive alternate therapeutic delivery strategy for the treatment of lung epithelium diseases.**
*Molecular Therapy–Nucleic Acids* (2013) **2**, e96; doi:10.1038/mtna.2013.22; published online 4 June 2013
**Subject Category:** siRNAs, shRNAs, and miRNAs; Nanoparticles

## Introduction

The pulmonary system is the primary site of entry and establishment of many airborne viral and bacterial pathogens as well as the site for a number of diseases such as asthma, chronic obstructive pulmonary diseases, tumor metastasis, and cystic fibrosis. The discovery and development of RNA interference technologies has resulted in a promising new therapy for a variety of diseases of the respiratory tract.[1]

However, the main barrier to the use of RNAi targeting pulmonary diseases is the absence of efficient delivery vectors, particularly in the diseased state.[2] The majority of studies have concentrated on the delivery of RNAi via inhalation as it has the benefits of being less invasive, avoids potential systemic toxicity and has increased specificity for the pulmonary system. However, intranasal delivery and inhalation techniques must overcome several biological barriers to enable sufficient delivery for target gene suppression. These barriers include the clearing sweeping motions of respiratory cilia as well as the mucous and pulmonary surfactant layer.[3] In addition, tissue inflammation and extensive deposition of extracellular matrix might hamper delivery to the lower respiratory tract potentially limiting the therapeutic use of inhalation delivery systems. Indeed, the modest efficacy of inhaled siRNA in clinical trials for the treatment of respiratory syncytial virus has been suggested to result from inefficient delivery during acute infection.[4,5]

An alternative route for pulmonary delivery is the intravenous (IV) route. IV liposome siRNA delivery to the steady state pulmonary environment has successfully shown the delivery and knockdown of endothelial-specific genes.[6,7] However, delivery to the lung epithelium via this method has historically been unsuccessful. Novel therapeutic strategies for the treatment of many diseases, such as viral infections or epithelial diseases would require efficient delivery to lung epithelial cells. Significant research has been conducted for the successful liposome delivery of RNAi to lung epithelial tumors.[8,9] However, the disrupted vascular architecture in a tumor environment limits the comparisons that can be made to normal pulmonary architecture and thus delivery. Polyethylenimines (PEI) have been used to protect siRNA molecules and achieve delivery to the lung epithelium via IV delivery.[10] However, PEI has been associated with pro-inflammatory responses[11–13] and toxicity upon multiple doses[14] thus reducing its potential for clinical use. Therefore, a novel approach for IV delivery of liposomes to lung epithelium is warranted for the treatment of pulmonary diseases.

In this report, we investigated the potential of stealth liposomes to achieve RNAi delivery to the lungs following IV injection. Liposome uptake was noted in lung endothelial and epithelial cells as well as leukocytes. We subsequently investigated the ability of our liposome siRNA delivery to achieve targeted knockdown of gene and protein expression in the lung and analyzed silencing in epithelial cells. To our knowledge, this is the first report which describes the systemic delivery of siRNAs to the epithelial cells of the lungs via cationic liposomes.

## Results

### Characterization of lipid nanoparticles and evaluation of *in vivo* biodistribution

We previously described a novel method of liposome formulation, the hydration of a freeze-dried matrix (HFDM) method.[15] We observed that IV injection of HFDM-formulated

[1]University of Queensland Diamantina Institute, Brisbane, Australia; [2]School of Veterinary Science, University of Queensland, Brisbane, Australia; [3]Department of Gynecologic Oncology, The University of Texas MD Anderson Cancer Center, Houston, Texas, USA; [4]Australian Infectious Diseases Research Centre, University of Queensland, Brisbane, Australia; [5]Griffith Health Institute and School of Medical Sciences, Griffith University, Southport, Australia. Correspondence: Nigel AJ McMillan, Griffith Health Institute and School of Medical Sciences, Griffith University, Southport, Queensland, Australia. E-mail: n.mcmillan@griffith.edu.au
**Keywords:** endothelial; epithelial; i*n vivo*; lung; siRNA; stealth liposome
Received 24 September 2012; accepted 28 March 2013; advance online publication 4 June 2013. doi:10.1038/mtna.2013.22

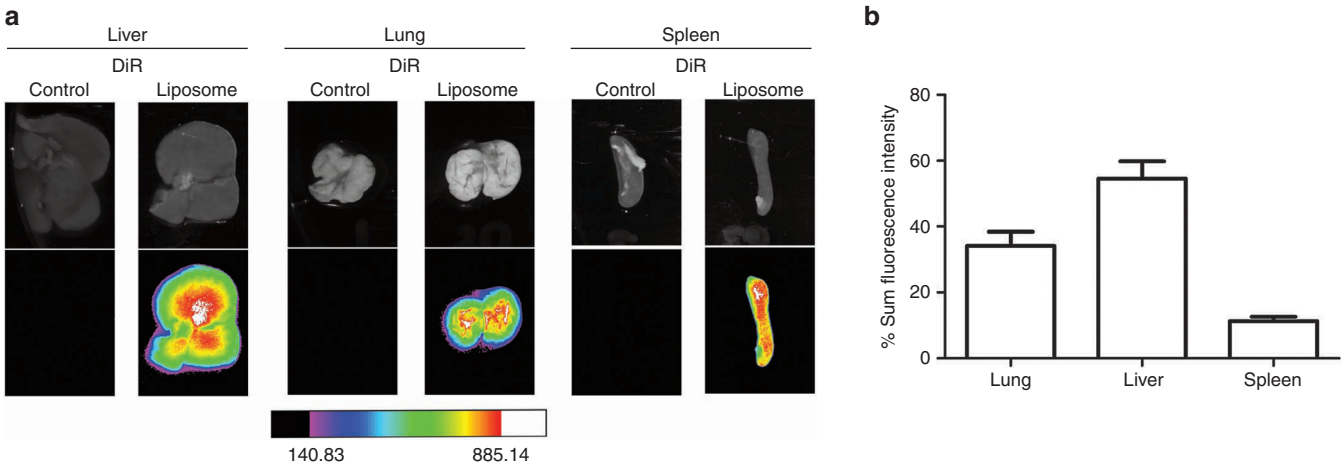


**Figure 1 Biodistribution of siRNA-loaded, DiR-labeled liposome nanoparticles after intravenous (IV) injection in mice.** (**a**) Livers, spleens, and lungs were removed 48 hours after IV administration and analyzed on the fluorescent imager (λex = 720 nm; λem = 790 nm). Scale shows intensity of DiR fluorescence. (**b**) Quantitative analysis of fluorescence intensity for each individual organ. Results are the mean ± SEM of $n = 6$ from two independent experiments.

liposomes containing N-[1-(2,3-dioleoyloxy)propyl]-N,N,N-trimethylammonium methyl-sulfate (DOTAP), cholesterol, 1,2-dioleoyl-sn-glycero-3-phosphoethanolamine (DOPE), polyethylene glycol (PEG) 2000-$C_{16}$Ceramide (50:35:5:10 molar ratio), and a lipophilic dye, DiR, showed significant accumulation in the lung, liver and spleen (**Figure 1a**). Minimal delivery of HFDM-formulated liposomes was seen in other organs such as the kidney, heart and bladder (data not shown). Of delivery to the three main organs, we observed that 34 ± 4% of the HFDM-formulated PEGylated lipid particles localized to the lung with further distribution to the liver (55 ± 5%) and spleen (11 ± 1%) (**Figure 1b**). This is consistent with previous reports using PEG-containing delivery systems.[16–20] It was unclear whether lung DiR accumulation resulted from liposome entrapment in the fine capillary beds, though further examination of delivery intensity throughout the lung (**Figure 1a**) suggested that the majority of delivery had uniform distribution. These observations lead us to investigate if these PEGylated liposomes could be used to deliver siRNA into the lung. We thus generated HFDM-prepared PEGylated siRNA containing particles. Upon rehydration the size, polydispersity index and zeta potential of the resulting lipid particles, as well as the entrapment efficiency of siRNA were measured (**Table 1**). The results showed that the liposomes have desirable characteristics for *in vivo* delivery including high entrapment efficiency and a size below 200 nm.[15]

**Table 1** Characterization of siRNA-loaded PEGylated lipid particles

| | |
|---|---|
| Size (nm)[a] | 190.25 ± 11.6 |
| Polydispersity index | 0.326 ± 0.03 |
| Zeta potential (mV) | 52.1 ± 0.832 |
| siRNA entrapment efficiency (%) | 94.8 ± 3.13 |

Each sample contained 40 µg siRNA in 300 µl isotonic sucrose solution. Three batches HFDM liposomes were analyzed ($n = 3$).
[a]Size represents $Z_{ave}$ ± SD as measured by Malvern Nano Zetasizer.

### Liposome treatment does not cause lung inflammation

It has been comprehensively shown that DOTAP in certain isomeric forms and concentrations can cause the production of reactive oxygen species and the activation of $CD8^+$ T cells.[21–23] Although these effects have been reported as beneficial in a tumor environment,[24,25] their induction in normal homeostasis or alternate disease models can cause significant damage. Our previous investigations of the HFDM liposomal formulation used here had determined that there were no significant increases in lactate dehydrogenase levels indicating liver toxicity or serum levels of inflammatory cytokines (interferon-α (IFNα), interleukin-6 (IL-6), and IFNγ) after IV treatment of mice.[26–28] To investigate this further, we performed hematoxylin and eosin staining of lung sections from mice treated intravenously with HFDM liposomes containing control and lamin siRNA at 48 hours after treatment, and compared them to untreated murine lungs (**Figure 2a,b**). In both ScrM7 and siLamin-treated mice, a transient low-grade vascular activation, including endothelial cell reactivity and increased neutrophil margination and adherence to endothelial cells was noted at 6 and 12 hours which resolved by 24–48 hours after treatment. This was a non-specific effect associated with the presence of HFDM liposomes themselves. Importantly, there was no evidence of inflammation, vascular activation, or leukocytic recruitment at the 48 hour time point. To confirm this at the molecular level, we undertook quantitative PCR (qPCR) of the inflammatory cytokines TNFα and IFNβ from treated and control lung tissue at various time points from 6 to 48 hours after treatment. A small (twofold) increase was observed in IFNβ levels at 6 hours in siLamin-treated animals but by 48 hours no significant changes in either cytokine were found. This suggests that the HFDM liposomes delivered intravenously, or siLamin itself, cause no significant immune activation in the lung.

### Cellular distribution in the lung

We examined which cell types in the lung were targeted and transfected by our HFDM liposomes. Mice were injected with DiR-labeled liposomes and at 48 hours lungs were removed and single cell suspensions were analyzed by flow cytometry.

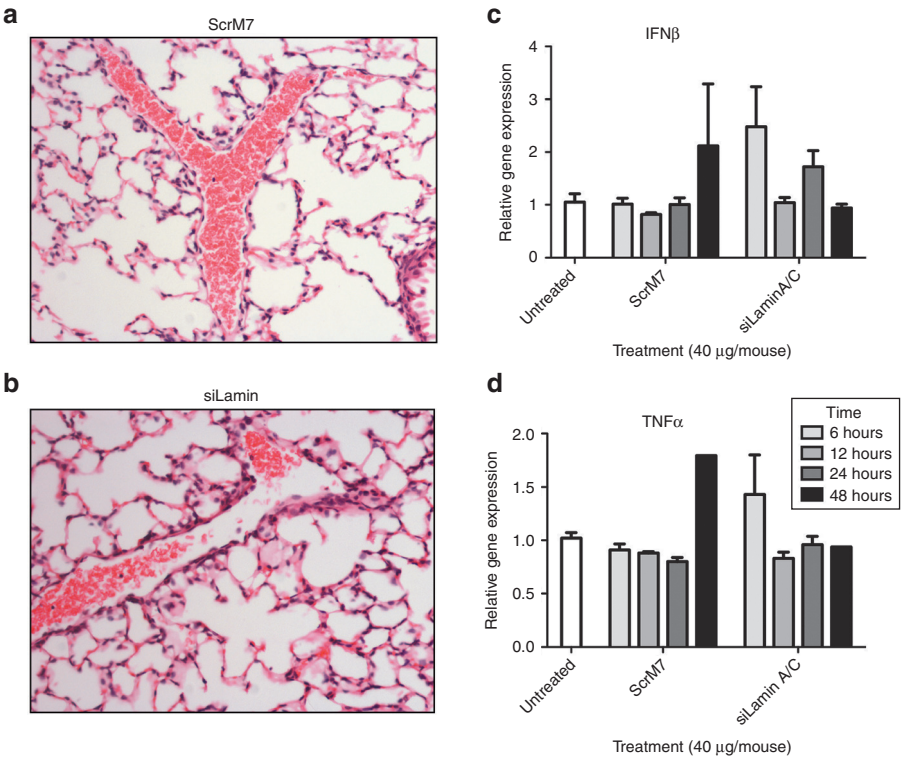


**Figure 2 Microscopic morphologic evaluation of murine lungs after liposome delivery.** Mice were injected with a single IV administration of either (**a**) scrambled control siRNA (ScrM7) or (**b**) siLamin containing liposomes. At 48 hours after injection, lung tissue was harvested, perfusion fixed, and routine histologic sections were stained with hematoxylin/eosin and imaged at 200×. To investigate inflammation at the molecular level, quantitative real-time PCR was carried to determine the levels of murine (**c**) IFNβ or (**d**) TNFα. Mice were treated with siRNA-loaded liposomes (control ScrM7 or siLamin) or untreated and total RNA extracted from lung tissue at the times indicated. Data shown are representative images from $n = 8$ mice per group from two independent experiments.

Of total lung cells, 47 ± 3% were positive for the fluorescent dye, DiR (**Figure 3a**). We next defined the individual cell populations using cell-specific markers (**Supplementary Figure S1**). A high proportion (64 ± 10%) of CD146$^+$ endothelial cells were DiR$^+$ (**Figure 3b**). This observation was expected as the endothelial cells would be exposed to IV delivery of liposomes via the pulmonary vasculature. Surprisingly, we also observed that 45 ± 7% of CD326$^+$ (epithelial cell adhesion molecule, EpCAM) cells were also positive for liposome delivery (**Figure 3b**). In humans, CD326 expression is restricted to epithelial cells, whereas in mice CD326 is expressed by epithelial cells and several leukocyte populations, including mononuclear phagocytes.[29] To further define liposomal epithelial cell delivery, we used the hematopoietic marker CD45 to differentiate CD326$^+$CD45$^-$ epithelial cells from CD326$^+$CD45$^+$ hematopoietic cells (**Figure 3c,d**). We observed that 23 ± 1% of CD326$^+$ cells were CD45$^+$ indicating that they were part of the hematopoietic linage. CD326$^+$CD45$^+$ hematopoietic cells were 42 ± 6% positive for liposome delivery. The other 76 ± 2% of CD326$^+$ cells were CD45$^-$ indicating that they were lung epithelial cells. CD326$^+$CD45$^-$ lung epithelial cells were 45 ± 1% positive for liposome delivery. Cationic liposomes have not previously been shown to transfect pulmonary epithelial cells, likely due to their tendency to aggregate, which we have shown does not occur in our particles due to PEGylation.[15]

### Immune cells also take up HFDM liposomes

Given the propensity for macrophages and monocytes to take up liposomes, we subsequently investigated the ability of immune cells within the lung and lung vasculature to become transfected. We used CD11b/CD11c, B220, and CD3 markers to distinguish general populations of myeloid, B lymphocytes and T lymphocytes respectively. We observed that 35 ± 7% and 29 ± 4% of CD11b$^+$ and CD11c$^+$ cells, 17 ± 3% of B220$^+$ cells and 8 ± 1% of CD3$^+$ cells were DiR$^+$ (**Figure 3c**). In addition, CD45$^+$ cells were 32 ± 1% positive for DiR liposome delivery (**Figure 3e**). As myeloid cells play a central role in the removal of foreign particles, we expected that the majority of systemically delivered particles would be taken up by these cells. In fact, cells of the myeloid lineage showed the highest liposomal delivery after IV injection in the spleen and liver (**Supplementary Figure S2**).

### Ability to deliver to epithelial and endothelial cells of the lower respiratory tract

To further confirm that the liposomes were delivered to epithelial cells within the lung, we performed confocal immunofluorescent microscopy. By using this method, we could examine if delivery was achieved in the small alveoli, bronchi and connecting vasculature or if it was contained to the large airways and blood vessels of the pulmonary system. In addition, we were able to further examine epithelial

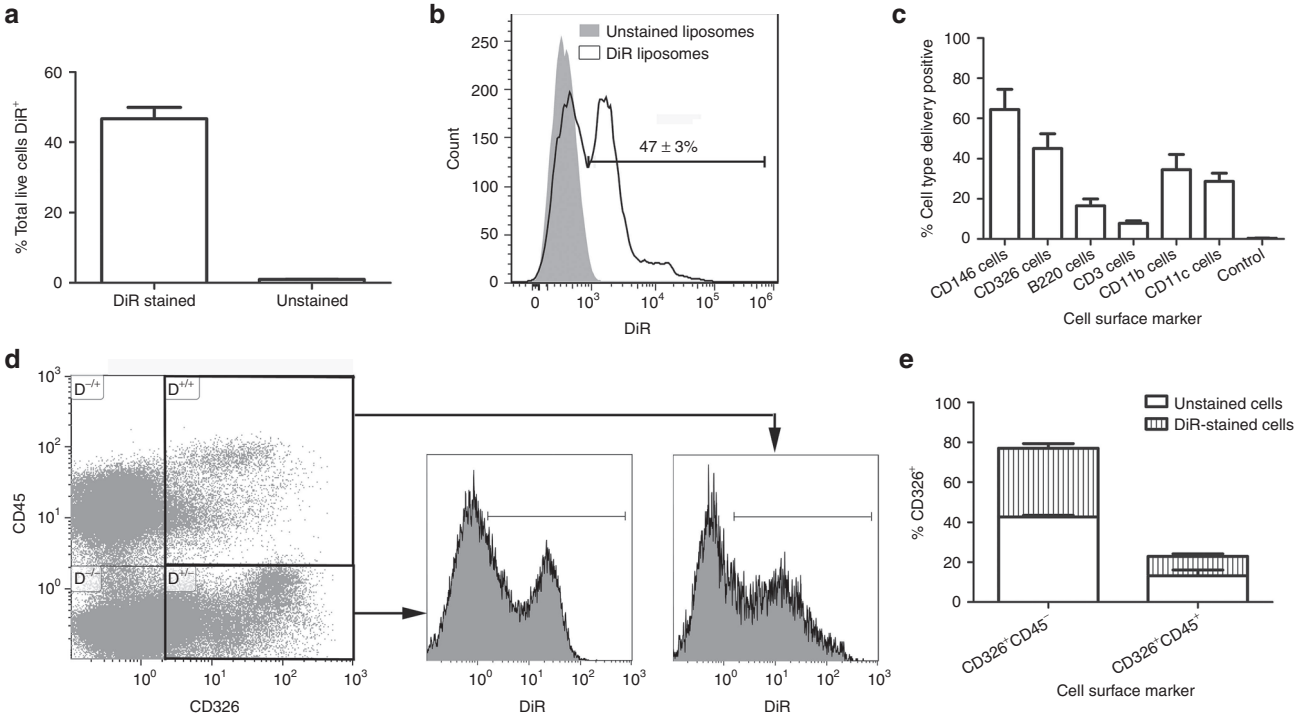


**Figure 3 Liposomal delivery to lung cells.** (**a**) Total lung cells were purified 48 hours after a single IV administration of unstained or DiR-stained liposomes. Cells were analyzed by flow cytometry. Delivery was quantified as a percentage of DiR$^+$ cells/total cells. Data shown are mean ± SEM of $n = 6$ mice per group analyzed in two independent experiments. (**b**) Representative FACS histogram of unstained and DiR-stained liposomes are shown. (**c**) Individual cell populations were analyzed by flow cytometry for DiR fluorescence. Delivery was quantified as a percentage of DiR$^+$ cells/total cells in the specific population. Control was mice treated with unstained liposomes. Data shown are mean ± SEM of $n = 6$ mice per group analyzed in two independent experiments. (**d**) Gating strategy for the analysis of CD45 and CD326$^+$ cell populations by flow cytometry. (**e**) Analysis of the CD326$^+$ cell population showing the level of DiR-stained liposome delivery to CD45$^-$ epithelial cells and CD45$^+$ immune cells. Delivery was quantified as the percentage of total cells in the specific population. Data shown are ± SEM of $n = 4$ mice per group from two independent experiments.

specific delivery rather than immune cell delivery. Markers for endothelial (CD146) and epithelial (CD326) cells were used to costain frozen lung sections 48 hours after IV delivery of a single liposome dose. Delivery to both epithelial and endothelial cells was confirmed with liposomes visualized in the small airways and blood vessels of the lower respiratory tract (**Figure 4a**). Upon higher magnification to further investigate CD326$^+$ epithelial cell delivery, we observed colocalization of DiR-stained liposomes and epithelial cells with distribution of liposome throughout epithelial cell surface and cytoplasm (**Figure 4d**).

To exclude passive transfer of the DiR fluorescent lipophilic dye, unlabeled liposomes were loaded with AlexaFluor-750-labeled siRNAs to confirm direct delivery to target cells. Confocal microscopy confirmed the presence of AlexaFluor-750-siRNAs in both CD146$^+$ endothelial and CD326$^+$ epithelial cells of the lung and thus validated delivery to these cell populations in the lung (**Figure 4b**).

### Potent silencing of gene targets in the lung after IV injection

After demonstrating successful delivery of siRNA to the lung using the PEG-liposomes, we examined whether this delivery resulted in functional gene silencing. We evaluated reductions in mRNA and protein levels of the ubiquitously expressed Lamin A/C. Mice were injected IV with 2 mg/kg of siRNA (~40 µg per dose per mouse) contained in PEG-liposomes. mRNA and protein expression of Lamin A/C were determined 48 hours after injection. We compared the impact of a previously validated Lamin A/C specific siRNA[30] versus animals injected with an identical formulation containing a control siRNA targeting either β-galactosidase[31] or a scrambled control.[26] 48 hours after single IV siRNA injection, we observed a significant reduction of Lamin A/C mRNA expression by 80 ± 0.1% in whole lung tissue (**Figure 5a**).

To examine the Lamin A/C protein, mice were injected with siRNA-containing PEG-liposomes on day 0 and 1 and protein expression of Lamin A/C in lungs was examined on day 4. This strategy was adopted as previous *in vitro* silencing of Lamin A/C indicated that significant reductions in protein levels were only seen after 48 hours.[32,33] Therefore, a 3-day interval between injection and protein level analysis was chosen to enable the reduction in mRNA levels to be translated into decreased Lamin A/C protein expression. We observed that Lamin A/C protein levels were significantly reduced in all mice that received LaminA/C siRNA, but not in untreated or control siRNA–treated mice (**Figure 5b,c**). Protein reductions in whole lung lysates from mice treated with the Lamin A/C specific siRNA indicated highly effective 55 ± 0.2% knockdown of Lamin A/C, thus corroborating the mRNA silencing results.

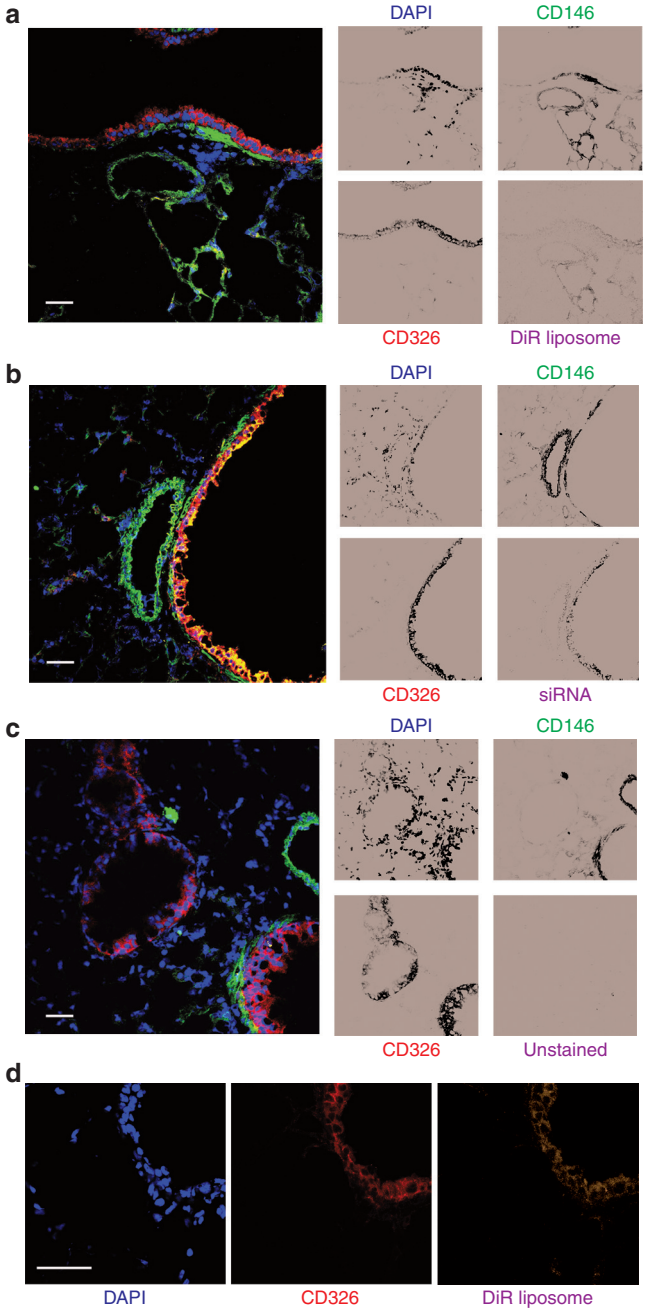


**Figure 4 Immunofluorescent evaluation of liposomal delivery to lung tissue.** Mice were injected with a single IV administration of (**a**,**d**) DiR-stained liposomes, (**b**) liposomes containing AF750 tagged siRNA, or (**c**) unstained liposomes. At 48 hours after injection, lung tissue was harvested, sectioned, and stained for CD146, CD326, and DAPI nuclear stain and analyzed via confocal microscopy. Scale bar represents 25 μm. Data shown are representative images from $n = 6$ mice per treatment group from three independent experiments.

### Gene silencing in epithelial and endothelial cells of the lung after IV injection

A key question for therapeutic gene silencing in the pulmonary system is whether silencing can be achieved in epithelial and endothelial cells that receive liposome delivery. Moreover, as epithelial cell delivery by cationic liposomes has not been previously reported, we sought to determine if siRNA was functional in these cells. Although the analysis of the entire pulmonary system showed high levels of gene silencing, it did not allow us to quantitate the level of silencing in each of these clinically relevant target cells. To address this, we injected a single 2 mg/kg dose of Lamin A/C siRNA IV in PEG-liposomes. At 48 hours, single cell suspensions of lungs were prepared and enriched for CD146$^+$ endothelial and CD326$^+$ epithelial cells via antibody mediated magnetic separation (**Supplementary Figure S3**). Lamin A/C mRNA expression was determined by quantitative real-time PCR (qRT-PCR). CD146$^+$ endothelial cells exhibited 49 ± 0.2% reduction in Lamin A/C mRNA expression when compared to control siRNA (**Figure 6a**). Similarly, CD326$^+$ cells achieved 54 ± 0.2% silencing of Lamin A/C mRNA (**Figure 6b**). The specific reduction of Lamin A/C mRNA in both CD326$^+$ and CD146$^+$ cells of the lungs indicated that delivery and functional silencing was achieved.

To provide direct evidence that the potent silencing of Lamin A/C was caused by the RNAi mRNA cleavage mechanism, we undertook a Taqman-based stem-loop RT-PCR assay to detect 5′ cleavage products predicted from Lamin A/C siRNA cleavage. This method uses a stem-loop primer that binds to the individual 5′ cleavage product at the 3′ cleavage site and primes reverse transcription (**Supplementary Figure S4**). To ensure that only the specific siRNA-generated cleavage was detected, we performed a Taqman PCR using Lamin A/C specific forward primer, a loop-specific reverse primer and a probe spanning the specific ligation site. Using this assay, we were able to detect the exclusive 5′ Lamin A/C cleavage product in the siLamin A/C liposome–treated CD146$^+$ and CD326$^+$ murine lung cells, and the positive control (**Figure 6c**). There was no amplification of the 5′ cleavage product was in either the control siRNA or untreated murine lung samples. Overall, the stem-loop Taqman qPCR analysis confirmed that the specific reduction of Lamin A/C mRNA was caused by the RNAi mechanism.

## Discussion

Here, we show for the first time that cationic liposomes are highly effective at transfecting not only endothelial cells but also epithelial cells of the lung following IV delivery. Moreover, this delivery was functional with 80% loss of mRNA and a 50% loss of target protein in lung tissue. For delivery of siRNA to the lung, many different routes using a diverse range of nanoparticles have been previously tested. These include intratracheal, intranasal, and IV delivery and each have shown varying degrees of success in mice and humans (reviewed in ref. 34). The most popular route is intranasal delivery where transfection of epithelial cells is achieved at high levels, although subsequent systemic circulation is poor and delivery of siRNAs into lung endothelial cells by this route has proven difficult. Furthermore, many obstructive barriers are present in intranasal delivery due to respiratory secretions, mucus, and cilia, which potentially limit access to target cells. This is particularly exacerbated in the diseased state. Indeed, this may be the reason for the diminished effectiveness of intranasal siRNA therapies targeting viruses

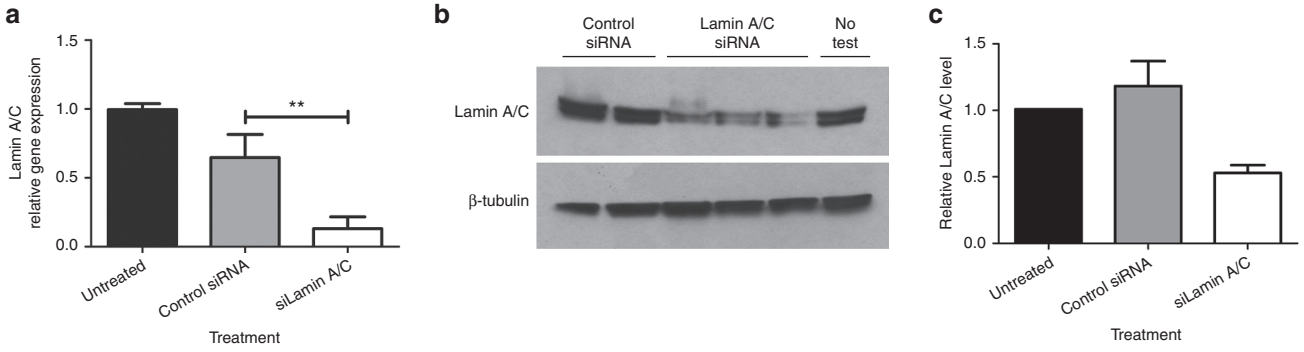


**Figure 5 siRNA liposome–mediated gene knockdown in murine lung cells *in vivo*.** (**a**) Lungs were collected at 48 hours after a single IV administration of Lamin A/C or control siRNA (40 µg, ~2.5 mg/kg). Gene expression levels of Lamin A/C were quantified by qRT-PCR as relative expression to β-actin housekeeping gene. Results are the mean ± SEM of $n = 9$ mice per group from three independent experiments. Significant differences between non-specific control and Lamin A/C siRNAs are indicated (**$P < 0.01$; Student's *t*-test). (**b**) Western blot analysis of Lamin A/C expression in whole lung tissue. Each lane represents the Lamin A/C level in the total lung tissue in each individual mouse. Mice received two doses of Lamin A/C or control siRNA (40 µg/dose) IV and were analyzed 4 days after initial injection. (**c**) Quantitative analysis of the combined LaminA and C protein levels between treatment and control groups. Results are the mean ± SEM of $n = 6$ mice per group from two independent experiments.

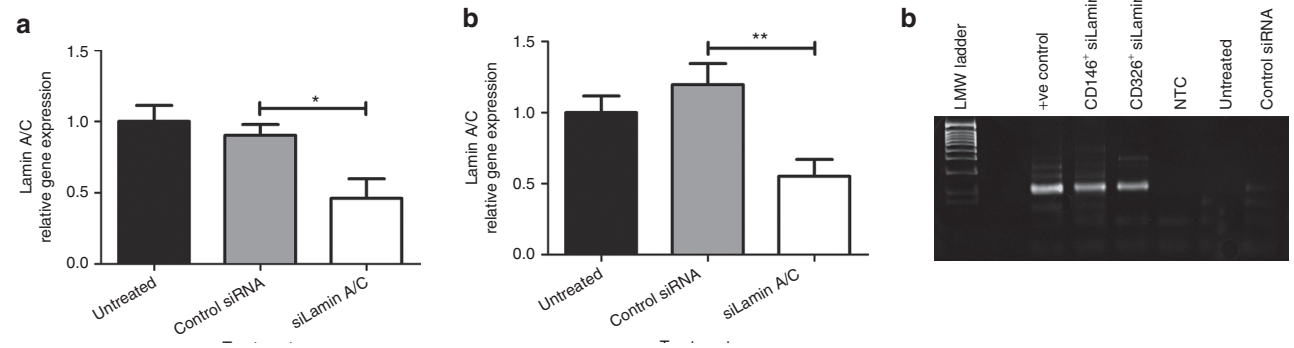


**Figure 6 Knockdown analysis of Lamin A/C in epithelial and endothelial cells.** Lungs were collected at 48 hours after a single IV administration of Lamin A/C or control siRNA (40 µg). Cell populations were enriched for CD146$^+$ and CD326$^+$ cells by MACS using positive selection. Gene expression levels of Lamin A/C in (**a**) CD146 and (**b**) CD326-enriched cell populations were quantified by qRT-PCR and are depicted as relative expression to β-actin. Results are the mean ± SEM of $n = 6$ from two independent experiments. Significant differences between non-specific control and Lamin A/C siRNAs are indicated (*$P < 0.05$, **$P < 0.01$; Student's *t*-test). (**c**) Stem-loop qPCR detection of 5′ Lamin A/C cleavage product in positive control, untreated mice lungs, CD146$^+$ and CD326$^+$ MACS-enriched cells from siLamin A/C or control siRNA–treated mouse lungs. Two mice per treatment were analyzed. The positive control sample was prepared by transfecting TC-1 cells with siLamin A/C for 24 hours. The template negative control (NTC) was prepared by incorporating all of the RT-PCR reagents except the cDNA template. LMW, low molecular weight; MACS, magnetic-activated cell sorting.

in the lung. For example, post-exposure therapies of siRNA for respiratory syncytial virus, typically only 4–24 hours after infection, resulted in significantly reduced effectiveness of the treatment of viral burden in the lung in a mouse model.[35] In lung transplant patients treated for respiratory syncytial virus with siRNA, little effect on viral burden was observed.[5] For influenza virus, intratracheal treatment using jetPEI/siRNA 5 hours after infection resulted in a 1,000-fold reduction in virus titers, but treatment 24 hours after infection only gave a twofold reduction, despite the high doses used in this study.[36] This suggests that significant loss of efficacy occurred due to impaired delivery.

Successful IV delivery to pulmonary endothelial cells has been well established (reviewed in ref. 7). However, this delivery route has thus far only resulted in little or no epithelial cell penetration. Limited transfection of large type 2 pneumocytes within lung epithelia were reported using PEI-conjugated plasmid DNA injected intravenously.[37] Cationic liposomes containing DODAC:DOPE (50:50) have previously been shown to efficiently transfect endothelial cells, macrophages and monocytes, but only rare delivery to epithelial cells was found.[38]

Therefore, in this present study, we investigated cationic stealth liposomes that were generated using our published HFDM method.[15] This is a simple method of formulating PEGylated siRNA-loaded lipid particles with characteristics favorable for *in vivo* delivery. The polydispersity index was consistent with our previous findings and, as expected, was higher than that of extruded particles.[15] We have previously shown that despite the positive zeta potential these particles do not induce liver toxicity[28] or inflammatory cytokine responses.[26,27] In this study, we have further shown that there was no morphologic evidence of inflammation, including immune cell infiltration, at 48 hours in liposome-treated

murine lungs, suggesting the treatment does not cause significant immune activation.

A potential reason that we observe siRNA transfection of epithelial cells with HFDM liposomes may be due to the combination of PEG stealth liposomes, together with the positive zeta potential. This would diminish uptake by professional phagocytes[39] and encourage interaction with negatively charged endothelial cells.[16] It is well known that intravenously delivered particles travel to the lungs and indeed 34 ± 4% of total liposomes were found to be lung associated at 48 hours. Liposomes distribute via the enhanced permeability and retention effect[40] and thus the majority of particles accumulate in the liver due to the fenestrated architecture of the blood vessels.[41,42] Cationic liposomes that use the enhanced permeability and retention effect for biodistribution must also use strategies that prevent aggregation of the delivery vector in the presence of serum. These include the use of a hydrophilic polymer, such as PEG, to shield the positive charge on the particle surface and inhibit interaction with cells of the reticulo-endothelial system. Still, a significant proportion of leukocytes had taken up labeled PEG-liposomes. The PEG-ceramide is known to dissociate from the liposome surface so this may explain the delivery to myeloid cells. However, non-targeting liposomes have previously thought to be inefficient for transfecting cells at sites other than liver. Our study now shows that lung endothelial and epithelial cells are proficiently transfected by a single dose of liposomes delivered via the IV route.

Our data demonstrates that cationic liposome-mediated siRNA delivery leads to transfection of epithelial cells beyond the endothelial barrier. Although the detailed molecular mechanisms by which this occurs remain to be determined, passive mechanisms of sequestration were eliminated due to the lack of diffused equal value delivery throughout every cell population of the lung. Thus, possible mechanisms of siRNA liposome positive sequestration may occur via direct cell contact with or exosomal transfer from transfected endothelial cells. Indeed, plants have been known to transmit dsRNA between cells[43] and recently, endogenus microRNAs have also been shown to be transmitted.[44–46] In mammalian cells, there is evidence to suggest cell-to-cell transfer of small RNAs via connexin-43-based gap junctions[47] in a range of cells, including cardiomyocytes,[47,48] bone-marrow stromal and tumor cells,[49] and glioma cells.[50] Evidence of *in vivo* transmission of small silencing RNA was recently shown between hepatic cells in a mouse liver.[51] In addition, direct transfection of epithelial cells may occur by liposomes gaining direct access to the alveolar space or by retransfection via endothelial cells. Further investigation is required to elucidate this mechanism.

Overall our data demonstrate that highly effective delivery of siRNA resulting in gene silencing in both endothelial and epithelial cells of the lung can be achieved using cationic liposomes via IV injection. We are presently investigating the significance of this in achieving gene knockdown in pathology conditions, including viral infections. The precise mechanism of how epithelial transfection occurs remains to be determined. However, one can envision that using this method may provide a more efficient means of treating diseased or infected lungs when compared to other routes of delivery.

## Materials and methods

*Antibodies and siRNAs.* Primary antibodies used in western blot were rabbit anti-mouse Lamin A/C (Cell Signaling Technology, Beverly, MA) and rabbit anti-mouse β-actin (Cell Signaling Technology) polyclonal antibodies. Secondary reagent was a goat anti-rabbit IgG HRP-linked polyclonal antibody (Sigma-Aldrich, St Louis, MO).

Directly conjugated monoclonal primary antibodies were used for flow cytometry; CD146-FITC (clone ME-9F1; BioLegend, San Diego, CA), CD326-PE (clone G8.8; BioLegend), CD11b-PE (clone M1/70; BD Pharmingen, San Jose, CA), CD11c-PE (clone N418; eBiosciences, San Diego, CA), CD3-PE (clone 145-2C11; eBiosciences), B220-FITC (clone RA3-6B2; BD Pharmingen), and CD45.2-FITC (clone 104; eBiosciences).

siRNAs used in this study were siLamin A/C[52] and siBgal924[31] obtained from Genesearch (Shanghai, China) and ScrM7[26] obtained from Integrated DNA Technologies (Coralville, IA).

*Transfection of TC-1 cells.* The murine epithelial cell line TC-1 (ATCC CRL-2785) was maintained in RPMI 1640 supplemented with 10% (v/v) heat inactivated fetal calf serum, 100 units/ml Penicillin G, 100 µg/ml Streptomycin sulphate and 2 mmol/l L-glutamine. TC-1 cells were cultured to 90% confluence in 12-well plates for 24 hours before transfection at 37 °C under a 5% $CO_2$/95% air atmosphere. Cells were transfected with 40 nmol/l siLamin A/C or control siRNA for 4 hours in OptiMem serum free media (Invitrogen, Carlsbad, CA) using Oligofectamine (Invitrogen) according to the manufacturers' guidelines. Cells were incubated in complete media for a further 24 hours before RNA purification.

*Formulation of lipid nanoparticles.* Liposomes were prepared via the HFDM method as described previously.[15] Briefly, DOTAP, DOPE, cholesterol, and PEG2000-$C_{16}$Ceramide were dissolved in 1 ml of tert-butanol at a molar ratio of 50:5:35:10. Forty micrograms of siRNA was added to 1 ml of 55.5 mg/ml filtered sucrose solution before mixing with the lipid solution. The resultant formulation was then snap-frozen and freeze-dried overnight (ALPHA 1–2 LDplus, Martin Christ, Germany) at –80 °C and <0.1 mbar. Freeze-dried matrix was then hydrated with sterile water before use to obtain a 300 µl isotonic sucrose solution.

*Nanoparticle characterization.* Size, polydispersity, and zeta potential of the resultant liposomes were measured using a Zetasizer Nano ZS (Malvern Instruments, Malvern, UK) following appropriate dilution in distilled water. Measurements were carried out at room temperature. Two size measurements were performed with 10 runs per measurement undertaken.

In vivo *delivery.* 1,1-dioctadecyl-3,3,3,3-tetramethylindotricarbocyanine iodide (DiR) (155 ng; Invitrogen) was dissolved in 10% ethanol. DiR of 155 ng in 1 µl was added to each nanoparticle formulation. Female C57BL/6 mice of 10–12 weeks old (Animal Resource Center, Perth, Australia) were injected intravenously via the tail vein with 300 µl of DiR-labeled PEGylated liposomes containing 40 µg of siRNA. At 24 hours after administration, each mouse was anaesthetized using isoflurane (Abbott, Kurnell, Australia). The biodistribution

of DiR-labeled PEGylated liposomes was examined with the Kodak In Vivo Imager (Carestream Health, Rochester, NY) using excitation and emission wavelengths of 720 and 790 nm, respectively. Results were analyzed using the Kodak molecular imaging software. At 48 hours after administration, mice were euthanized and the lungs, liver, and spleen were removed, washed in phosphate-buffered saline (PBS) and examined via the Kodak In Vivo Imager. All experiments were approved by the University of Queensland Animal Ethics Committee.

*Flow cytometry.* Organs were removed and digested with collagenase D (1 mg/ml; Worthington Biochemical, Lakewood, NJ) and DNAseI (0.1 mg/ml; Roche Diagnostics, Indianapolis, IN) and passed through a 70 µm cell strainer (BD Biosciences, North Ryde, Australia) to obtain single cell suspensions. Cells were resuspended in PBS, 10% fetal calf serum, 10 mmol/l EDTA at a concentration of 0.5–1 × $10^7$ cells/ml and 1 µg/ml anti-mouse Fcγ receptor II/IIIFc Block (clone 2.4G2; BD Pharmingen) for 30 minutes at 4 °C, washed and stained with Aqua amine-reactive viability dye (Invitrogen) and fluorescently labeled specific antibodies at 4 °C for 30 minutes. After staining, the cells were washed twice with PBS, 10% fetal calf serum, 10 mmol/l EDTA and fixed in 4% paraformaldehyde. Cells were analyzed using a Gallios Flow Cytometer (Beckman Coulter, Brea, CA) and Kaluza flow cytometry software (Beckman Coulter).

*Histological analysis.* Lungs were perfused and fixed overnight in 10% neutral buffered formalin, prior to embedding in paraffin wax, sectioning at 5 µm and staining with Harris hematoxylin and eosin by routine histological methods. Four serial sections from each mouse were evaluated by light microscopy by a board-certified veterinary pathologist (RA) with extensive experience in laboratory animal tissue analysis. Tissues observed in all mice included lung, heart, mediastinum, thymus, and oesophagus.

*Immunofluorescence microscopy.* Lungs were perfused with optimal cutting temperature (OCT) compound:PBS (1:1) solution, placed in Tissue-Tek OCT compound and snap frozen in a dry-ice ethanol bath. Sections (10 µm) were then cut using a cryostat (Leica Microsystems, Wetzlar, Germany) and were mounted on Superfrost/Plus microscope slides (Fisher Scientific, Pittsburgh, PA).

Tissue sections were air dried for 1 hour and then fixed in ice-cold acetone for 5 minutes. Three PBS washes were used to remove the residual acetone and sections were placed in a humid chamber. Sections were blocked with 1% bovine serum albumin (Sigma-Aldrich)/5% normal rat serum in PBS for 15 minutes. Blocking solution was subsequently removed and primary antibodies (diluted in blocking solution) were incubated with the sections for 60 minutes. Sections were washed three times in PBS and a coverslip with Prolong gold antifade mounting reagent (Invitrogen) and DAPI nuclear stain (1:1,000) was applied. Images were obtained with a Zeiss LSM 510 Meta Confocal microscope using Zen 2008 software (Carl Zeiss, Oberkochen, Germany).

In vivo *knockdown.* Liposomes were prepared via the HFDM method containing control or Lamin A/C targeting siRNAs. Female C57BL/6 mice of 10–12 weeks old (Animal Resource Center) were injected IV via the tail vein with 300 µl of stealth liposomes containing 40 µg of siRNA. At 48 hours after administration, each mouse was euthanized and the lungs were removed, washed in PBS and processed for mRNA analysis. For protein analysis, mice had an additional stealth liposome IV injection at 24 hours and were processed at 72 hours after administration.

*Magnetic-activated cell sorting.* Cell populations from single cell suspensions were enriched by magnetic-activated cell sorting (MACS). Briefly, cells were stained with FITC and PE fluorescently labeled specific antibodies for CD146 and CD326 cells respectively. The cells were subsequently labeled with Anti-FITC and Anti-PE microbeads (MiltenyiBiotec, Cologne, Germany) and loaded onto an autoMACS column. Purified CD146 and CD326 cells were obtained using positive selection and cellular composition was determined before and after enrichment by flow cytometry.

For gene expression studies, cells were lysed in Trizol (Invitrogen). For western blot, cells were lysed with a 25 gauge needle in RIPA buffer containing protease inhibitor cocktail (Sigma-Aldrich) and 1 mmol/l PMSF.

*qRT-PCR, stem-loop PCR, and western blot.* Total RNA was purified using standard protocols (Invitrogen). Total RNA of 0.5–2 µg was used for reverse transcription (RT) using an Omniscript RT kit (Qiagen, Valencia, CA) as per the manufacturer's instructions. qPCR was performed in duplicate using the Rotor-gene system (Qiagen) using GoTaq qPCR SyBr green mix (Promega, Alexandria, New South Wales, Australia). ΔCt of the gene of interest was compared to the ΔCt of the reference gene to determine relative gene expression. Gene of interest primers were specific for murine Lamin A/C, 5′-GAGAGGCTAAGAAGCAGC-3′ (sense) and 5′-ACGCAGTTCCTCGCTGTAA-3′ (antisense),[53] murine TNFα, 5′-CATCTTCTCAAAATTCGAGTGACAA-3′ (sense) and 5′-TGGGAGTAGACAAGGTACAACCC-3′ (antisense), murine IFNβ, 5′-AGCTCCAAGAAAGGACGAACAT-3′ (sense) and 5′-GCCCTGTAGGTGAGGTTGATCT-3′ (antisense), whereas reference gene primers were specific for murine β-actin, 5′-GCTACAGCTTCACCACCACA-3′ (sense) and 5′-TCTCCAGGGAGGAAGAGGAT-3′ (antisense).

For stem-loop PCR analysis, a Taqman-based stem-loop RT-PCR assay for detection of 5′ cleavage product was adapted from the protocol described by Chen and colleagues.[54,55] Total RNA of 500 ng was reverse transcribed with 1X RT buffer, 0.25 mmol/l dNTPs, 0.3 U/µOmniscript RT, 0.25 U/µl RNase inhibitor, and 50 nmol/l Lamin A/C cleavage stem-loop RT primer 5′-GTCGTATCCAGTGCAGG GTCCGAGGTATTCGCACTGGATACGACGGAAGT-3′. The RT reaction was incubated initially for 30 minutes at 16 °C, then for 30 minutes at 42 °C followed by 5 minutes at 85 °C and finally held at 4 °C. The RT reaction was subjected to a standard Taqman PCR assay which comprised 1 µl of RT product, 1X Taqman universal PCR master mix, 0.2 µmol/l Taqman probe 5′-6-FAM-ATGCTGAGGCGAGTGGATGCTG-3′ Black Hole Quencher 1 (Integrated DNA technologies), 1.5 µmol/l forward murine Lamin A/C primer 5′-CCTGGGAGAGGCTAAGAAGC-3′, and 0.7 µmol/l reverse loop–specific primer 5′-GGATACGACGGAAGTCAAGC-3′. The qPCR was performed on an Applied Biosystems 7900HT real-time PCR system (Life Technologies, New York, NY) at

95 °C for 10 minutes, followed by 40 cycles of 95 °C for 15 seconds and 60 °C for 1 minutes.

For western blot analyzes, total cell lysates were separated by sodium dodecyl sulphate polyacrylamide gel electrophoresis (SDS-PAGE) and transferred to Polyvinylidene difluoride membranes (Sigma-Aldrich) using a Trans-Blot System (Bio-Rad, Hercules, CA). Membranes were blocked in Tris-buffered saline containing 0.5% Tween and 5% milk powder for 2 hours at room temperature. Primary antibody binding was achieved overnight at 4 °C, whereas HRP-linked secondary antibody binding was achieved in 1 hour at room temperature. Enhanced chemiluminescence was used for visualization.

*Statistical analysis.* Groups were compared using two-sided Student *t*-test. *P* values of <0.05 were considered to be statistically significant.

### Supplementary material

**Figure S1.** Liposomal delivery to pulmonary epithelial and endothelial cells.
**Figure S2.** Intravenous liposomal delivery to the spleen and liver.
**Figure S3.** Purification of epithelial and endothelial cells.
**Figure S4.** Schematic diagram depicting Taqman-based stem-loop RT-PCR strategy.

**Acknowledgments.** We thank Sandrine Roy (UQ Diamantina Institute) for assistance with fluorescence microscopy and Kim Woolley, Norliana Kharruddin, and Allison Choyce for expert technical assistance. This work was supported by grants from the National Health and Medical Research Council (APP631402, APP1040904), and the Cancer Council of Queensland. J.M. was supported by UQ Diamantina Institute and Australian Postgraduate Award (APA). A.B. is supported by Fellowships funded by the Balzan Foundation and the University of Queensland (grant 2009001743). The authors declare no conflict of interest.

1. Rettig, GR and Behlke, MA (2012). Progress toward in vivo use of siRNAs-II. *Mol Ther* **20**: 483–512.
2. Lam, JK, Liang, W and Chan, HK (2012). Pulmonary delivery of therapeutic siRNA. *Adv Drug Deliv Rev* **64**: 1–15.
3. Merkel, OM and Kissel, T (2012). Nonviral pulmonary delivery of siRNA. *Acc Chem Res* **45**: 961–970.
4. DeVincenzo, J, Lambkin-Williams, R, Wilkinson, T, Cehelsky, J, Nochur, S, Walsh, E *et al.* (2010). A randomized, double-blind, placebo-controlled study of an RNAi-based therapy directed against respiratory syncytial virus. *Proc Natl Acad Sci USA* **107**: 8800–8805.
5. Zamora, MR, Budev, M, Rolfe, M, Gottlieb, J, Humar, A, Devincenzo, J *et al.* (2011). RNA interference therapy in lung transplant patients infected with respiratory syncytial virus. *Am J Respir Crit Care Med* **183**: 531–538.
6. Gutbier, B, Kube, SM, Reppe, K, Santel, A, Lange, C, Kaufmann, J *et al.* (2010). RNAi-mediated suppression of constitutive pulmonary gene expression by small interfering RNA in mice. *Pulm Pharmacol Ther* **23**: 334–344.
7. Kuruba, R, Wilson, A, Gao, X and Li, S (2009). Targeted delivery of nucleic-acid-based therapeutics to the pulmonary circulation. *AAPS J* **11**: 23–30.
8. Li, SD, Chono, S and Huang, L (2008). Efficient oncogene silencing and metastasis inhibition via systemic delivery of siRNA. *Mol Ther* **16**: 942–946.
9. Li, SD and Huang, L (2006). Targeted delivery of antisense oligodeoxynucleotide and small interference RNA into lung cancer cells. *Mol Pharm* **3**: 579–588.
10. Günther, M, Lipka, J, Malek, A, Gutsch, D, Kreyling, W and Aigner, A (2011). Polyethylenimines for RNAi-mediated gene targeting in vivo and siRNA delivery to the lung. *Eur J Pharm Biopharm* **77**: 438–449.
11. Gautam, A, Densmore, CL and Waldrep, JC (2001). Pulmonary cytokine responses associated with PEI-DNA aerosol gene therapy. *Gene Ther* **8**: 254–257.
12. Regnström, K, Ragnarsson, EG, Köping-Höggård, M, Torstensson, E, Nyblom, H and Artursson, P (2003). PEI - a potent, but not harmless, mucosal immuno-stimulator of mixed T-helper cell response and FasL-mediated cell death in mice. *Gene Ther* **10**: 1575–1583.
13. Rudolph, C, Lausier, J, Naundorf, S, Müller, RH and Rosenecker, J (2000). In vivo gene delivery to the lung using polyethylenimine and fractured polyamidoamine dendrimers. *J Gene Med* **2**: 269–278.
14. Merkel, OM, Beyerle, A, Beckmann, BM, Zheng, M, Hartmann, RK, Stöger, T *et al.* (2011). Polymer-related off-target effects in non-viral siRNA delivery. *Biomaterials* **32**: 2388–2398.
15. Wu, SY, Putral, LN, Liang, M, Chang, HI, Davies, NM and McMillan, NA (2009). Development of a novel method for formulating stable siRNA-loaded lipid particles for in vivo use. *Pharm Res* **26**: 512–522.
16. Santel, A, Aleku, M, Keil, O, Endruschat, J, Esche, V, Fisch, G *et al.* (2006). A novel siRNA-lipoplex technology for RNA interference in the mouse vascular endothelium. *Gene Ther* **13**: 1222–1234.
17. Svensson, RU, Shey, MR, Ballas, ZK, Dorkin, JR, Goldberg, M, Akinc, A *et al.* (2008). Assessing siRNA pharmacodynamics in a luciferase-expressing mouse. *Mol Ther* **16**: 1995–2001.
18. Watanabe, T, Umehara, T, Yasui, F, Nakagawa, S, Yano, J, Ohgi, T *et al.* (2007). Liver target delivery of small interfering RNA to the HCV gene by lactosylated cationic liposome. *J Hepatol* **47**: 744–750.
19. Yano, J, Hirabayashi, K, Nakagawa, S, Yamaguchi, T, Nogawa, M, Kashimori, I *et al.* (2004). Antitumor activity of small interfering RNA/cationic liposome complex in mouse models of cancer. *Clin Cancer Res* **10**: 7721–7726.
20. Zimmermann, TS, Lee, AC, Akinc, A, Bramlage, B, Bumcrot, D, Fedoruk, MN *et al.* (2006). RNAi-mediated gene silencing in non-human primates. *Nature* **441**: 111–114.
21. Dokka, S, Toledo, D, Shi, X, Castranova, V and Rojanasakul, Y (2000). Oxygen radical-mediated pulmonary toxicity induced by some cationic liposomes. *Pharm Res* **17**: 521–525.
22. Vasievich, EA, Chen, W and Huang, L (2011). Enantiospecific adjuvant activity of cationic lipid DOTAP in cancer vaccine. *Cancer Immunol Immunother* **60**: 629–638.
23. Yan, W, Chen, W and Huang, L (2007). Mechanism of adjuvant activity of cationic liposome: phosphorylation of a MAP kinase, ERK and induction of chemokines. *Mol Immunol* **44**: 3672–3681.
24. Chen, W, Yan, W and Huang, L (2008). A simple but effective cancer vaccine consisting of an antigen and a cationic lipid. *Cancer Immunol Immunother* **57**: 517–530.
25. Whitmore, M, Li, S and Huang, L (1999). LPD lipopolyplex initiates a potent cytokine response and inhibits tumor growth. *Gene Ther* **6**: 1867–1875.
26. Khairuddin, N, Gantier, MP, Blake, SJ, Wu, SY, Behlke, MA, Williams, BR *et al.* (2012). siRNA-induced immunostimulation through TLR7 promotes antitumoral activity against HPV-driven tumors in vivo. *Immunol Cell Biol* **90**: 187–196.
27. McCaskill, J, Wu, S, Khairuddin, N and McMillan, NAJ (2013). Lowering the siRNA delivery barrier: alginate scaffolds and immune stimulation. In Peer, D (eds). Nanotechnology for Delivery of DNA and Related Materials. Pan Stanford Publishing Pte. Ltd.: Singapore.
28. Wu, SY, Singhania, A, Burgess, M, Putral, LN, Kirkpatrick, C, Davies, NM *et al.* (2011). Systemic delivery of E6/7 siRNA using novel lipidic particles and its application with cisplatin in cervical cancer mouse models. *Gene Ther* **18**: 14–22.
29. Trzpis, M, McLaughlin, PM, de Leij, LM and Harmsen, MC (2007). Epithelial cell adhesion molecule: more than a carcinoma marker and adhesion molecule. *Am J Pathol* **171**: 386–395.
30. Elbashir, SM, Harborth, J, Lendeckel, W, Yalcin, A, Weber, K and Tuschl, T (2001). Duplexes of 21-nucleotide RNAs mediate RNA interference in cultured mammalian cells. *Nature* **411**: 494–498.
31. Judge, AD, Sood, V, Shaw, JR, Fang, D, McClintock, K and MacLachlan, I (2005). Sequence-dependent stimulation of the mammalian innate immune response by synthetic siRNA. *Nat Biotechnol* **23**: 457–462.
32. Harborth, J, Elbashir, SM, Vandenburgh, K, Manninga, H, Scaringe, SA, Weber, K *et al.* (2003). Sequence, chemical, and structural variation of small interfering RNAs and short hairpin RNAs and the effect on mammalian gene silencing. *Antisense Nucleic Acid Drug Dev* **13**: 83–105.
33. Banaszynski, LA, Chen, LC, Maynard-Smith, LA, Ooi, AG and Wandless, TJ (2006). A rapid, reversible, and tunable method to regulate protein function in living cells using synthetic small molecules. *Cell* **126**: 995–1004.
34. Roy, I and Vij, N (2010). Nanodelivery in airway diseases: challenges and therapeutic applications. *Nanomedicine* **6**: 237–244.
35. Bitko, V, Musiyenko, A, Shulyayeva, O and Barik, S (2005). Inhibition of respiratory viruses by nasally administered siRNA. *Nat Med* **11**: 50–55.
36. Ge, Q, Filip, L, Bai, A, Nguyen, T, Eisen, HN and Chen, J (2004). Inhibition of influenza virus production in virus-infected mice by RNA interference. *Proc Natl Acad Sci USA* **101**: 8676–8681.
37. Goula, D, Benoist, C, Mantero, S, Merlo, G, Levi, G and Demeneix, BA (1998). Polyethylenimine-based intravenous delivery of transgenes to mouse lung. *Gene Ther* **5**: 1291–1295.
38. Liu, Y, Mounkes, LC, Liggitt, HD, Brown, CS, Solodin, I, Heath, TD *et al.* (1997). Factors influencing the efficiency of cationic liposome-mediated intravenous gene delivery. *Nat Biotechnol* **15**: 167–173.
39. Allen, TM, Hansen, C, Martin, F, Redemann, C and Yau-Young, A (1991). Liposomes containing synthetic lipid derivatives of poly(ethylene glycol) show prolonged circulation half-lives in vivo. *Biochim Biophys Acta* **1066**: 29–36.
40. Maeda, H, Wu, J, Sawa, T, Matsumura, Y and Hori, K (2000). Tumor vascular permeability and the EPR effect in macromolecular therapeutics: a review. *J Control Release* **65**: 271–284.
41. Huang, L and Liu, Y (2011). In vivo delivery of RNAi with lipid-based nanoparticles. *Annu Rev Biomed Eng* **13**: 507–530.

42. Litzinger, DC, Brown, JM, Wala, I, Kaufman, SA, Van, GY, Farrell, CL *et al.* (1996). Fate of cationic liposomes and their complex with oligonucleotide in vivo. *Biochim Biophys Acta* **1281**: 139–149.
43. Brosnan, CA and Voinnet, O (2011). Cell-to-cell and long-distance siRNA movement in plants: mechanisms and biological implications. *Curr Opin Plant Biol* **14**: 580–587.
44. Carlsbecker, A, Lee, JY, Roberts, CJ, Dettmer, J, Lehesranta, S, Zhou, J *et al.* (2010). Cell signalling by microRNA165/6 directs gene dose-dependent root cell fate. *Nature* **465**: 316–321.
45. Dunoyer, P, Schott, G, Himber, C, Meyer, D, Takeda, A, Carrington, JC *et al.* (2010). Small RNA duplexes function as mobile silencing signals between plant cells. *Science* **328**: 912–916.
46. Molnar, A, Melnyk, CW, Bassett, A, Hardcastle, TJ, Dunn, R and Baulcombe, DC (2010). Small silencing RNAs in plants are mobile and direct epigenetic modification in recipient cells. *Science* **328**: 872–875.
47. Valiunas, V, Polosina, YY, Miller, H, Potapova, IA, Valiuniene, L, Doronin, S *et al.* (2005). Connexin-specific cell-to-cell transfer of short interfering RNA by gap junctions. *J Physiol (Lond)* **568**(Pt 2): 459–468.
48. Hosoda, T, Zheng, H, Cabral-da-Silva, M, Sanada, F, Ide-Iwata, N, Ogórek, B *et al.* (2011). Human cardiac stem cell differentiation is regulated by a mircrine mechanism. *Circulation* **123**: 1287–1296.
49. Lim, PK, Bliss, SA, Patel, SA, Taborga, M, Dave, MA, Gregory, LA *et al.* (2011). Gap junction-mediated import of microRNA from bone marrow stromal cells can elicit cell cycle quiescence in breast cancer cells. *Cancer Res* **71**: 1550–1560.
50. Katakowski, M, Buller, B, Wang, X, Rogers, T and Chopp, M (2010). Functional microRNA is transferred between glioma cells. *Cancer Res* **70**: 8259–8263.
51. Pan, Q, Ramakrishnaiah, V, Henry, S, Fouraschen, S, de Ruiter, PE, Kwekkeboom, J *et al.* (2012). Hepatic cell-to-cell transmission of small silencing RNA can extend the therapeutic reach of RNA interference (RNAi). *Gut* **61**: 1330–1339.
52. Harborth, J, Elbashir, SM, Bechert, K, Tuschl, T and Weber, K (2001). Identification of essential genes in cultured mammalian cells using small interfering RNAs. *J Cell Sci* **114**(Pt 24): 4557–4565.
53. Zhang, Y, Cristofaro, P, Silbermann, R, Pusch, O, Boden, D, Konkin, T *et al.* (2006). Engineering mucosal RNA interference in vivo. *Mol Ther* **14**: 336–342.
54. Chen, C, Ridzon, DA, Broomer, AJ, Zhou, Z, Lee, DH, Nguyen, JT *et al.* (2005). Real-time quantification of microRNAs by stem-loop RT-PCR. *Nucleic Acids Res* **33**: e179.
55. Cheng, A, Li, M, Liang, Y, Wang, Y, Wong, L, Chen, C *et al.* (2009). Stem-loop RT-PCR quantification of siRNAs in vitro and in vivo. *Oligonucleotides* **19**: 203–208.



Supplementary Information accompanies this paper on the Molecular Therapy–Nucleic Acids website (http://www.nature.com/mtna)